

Parallel multiscale simulation of hypersonic flow with porous wall injection

Adriano Cerminara, Ralf Deiterding,

Neil Sandham

Department of Aerospace Engineering,
University of Southampton

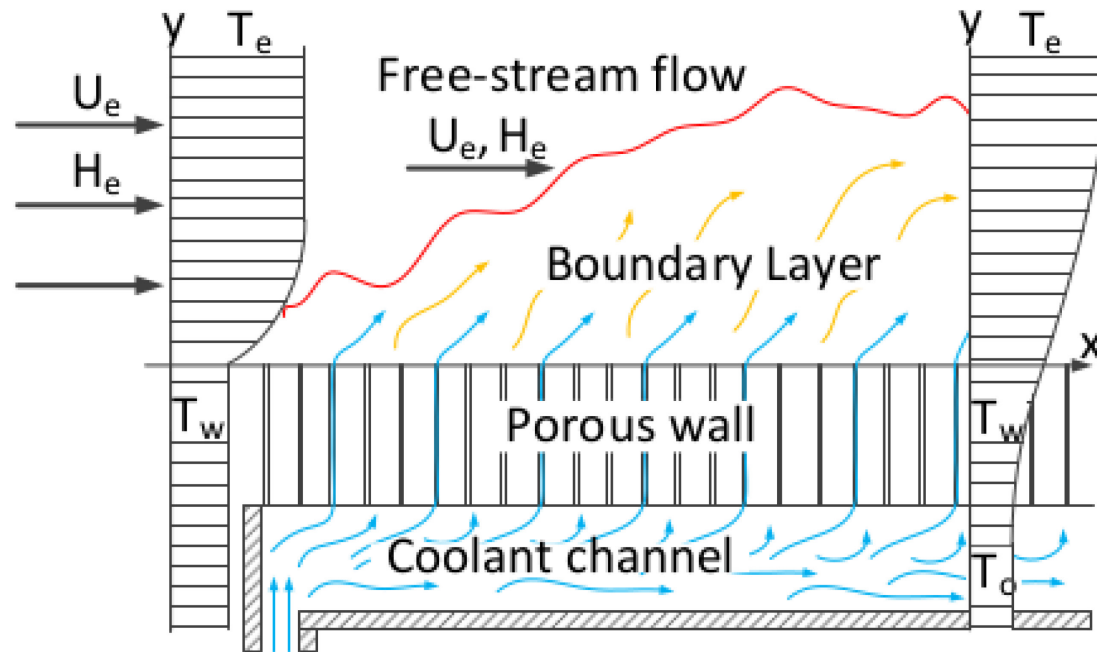
Pecs, 5/6/2019

Contents

- Introduction
- Numerical method
- 2D Flat plate – effect of plenum pressure
- 3D Flat plate – transition to turbulence
- Prototype porous structures
- Conclusions
- Part of EPSRC Programme Grant *Transpiration Cooling Systems for Jet Engine Turbines and Hypersonic Flight*
<http://transpirationcooling.eng.ox.ac.uk>

Introduction

- Understand the physics of blowing in hypersonic flow through porous surfaces
- Predict cooling performance – heat transfer rates
- Estimate the effects on BL stability and transition
- Validate results with experiments



Numerical method for full Navier-Stokes equations

- **Hybrid WENO-CD** method up to **6th -order** accurate for both inviscid and viscous fluxes (Cerminara, Deiterding, Sandham, 2018)
- Central Differencing (CD) scheme used in the smooth regions:
- E.g. for 6th -order, the numerical flux at the interfaces is evaluated as

$$\hat{f}_{i+\frac{1}{2}} = \alpha(f_{i+3} + f_{i-2}) + \beta(f_{i+2} + f_{i-1}) + \gamma(f_i + f_{i+1})$$

$$\alpha = 1/60 \quad \beta = -2/15 \quad \gamma = 37/60$$

- 3rd -order Runge-Kutta for time integration
- **Characteristic-based switch** to a high-resolution WENO scheme to handle discontinuities in a computationally efficient way (Hill and Pullin 2004)
- **Finite volume** approach in a Cartesian reference system
- Structured-adaptive-mesh-refinement (**SAMR**) algorithm (Deiterding 2005): the grid is **locally refined** by adding consecutive finer grid levels during the iteration cycles (patch-wise refinement strategy)

Numerical method - shock-capturing scheme

- Weighted-essentially-non-oscillatory - symmetric - order-optimized (**WENO-SYMOO**) scheme (Martin et al. 2006)
- **Reduced dissipation** (compared to 5th-order WENO-JS, Jiang and Shu 1996), and **6th** maximum formal **order** of accuracy, reached through:
 1. Symmetrization: a **fourth** candidate **stencil** is **added** to the initial ($r=3$)-points upwinded-biased candidate stencils of the WENO-JS
 2. Optimal weights C_k to guarantee 6th-order accuracy

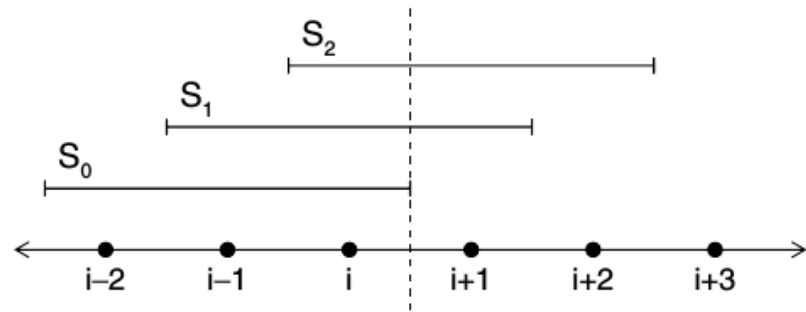
$$\hat{f}_{i+\frac{1}{2}}^+ = \sum_{k=0}^r \omega_k q_k^r \quad q_k^r = \sum_{l=0}^{r-1} d_{k,l}^r f(u_{i-r+k+l+1})$$

r-th-order polynomial interpolation on the k-th stencil

$$\omega_k = \frac{\alpha_k}{\sum_{k=0}^{r-1} \alpha_k} \quad \text{weight of the k-th interp.} \quad \alpha_k = \frac{C_k}{(\epsilon + IS_k)^p}$$

$$IS_k = \sum_{m=1}^{r-1} \left(\sum_{l=0}^{r-1} b_{k,m,l}^r f(u_{i-r+k+l+1}) \right)^2$$

smoothness indicator



from Martin et al. 2006

Numerical method - WENO-CD switch

- Riemann problem is solved at each cell interface through Roe's averaged state
- Lax condition is applied to detect shock/rarefaction waves

$$|u_R \pm a_R| < |u^* \pm a^*| < |u_L \pm a_L|$$

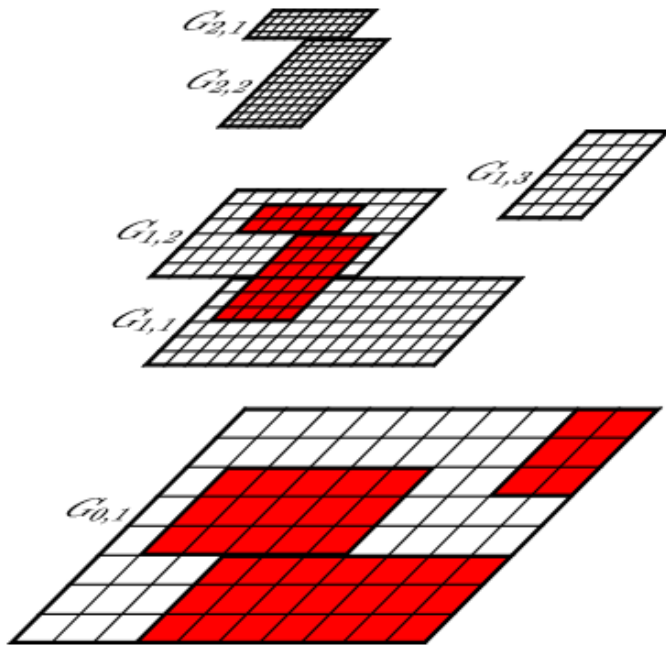
- A threshold is applied to the residuals between the left/right state and the intermediate state to select the strong waves and neglect the weak ones (Ziegler et al. 2011)
- Another threshold is applied to the function $\phi(\theta_i)$ to allow WENO only in the high pressure-gradient regions (Ziegler et al. 2011):

$$\phi(\theta_i) = \frac{2\theta_i}{(1 + \theta_i)^2} \quad \theta_i = \frac{|p_{i+1} - p_i|}{|p_{i+1} + p_i|}$$

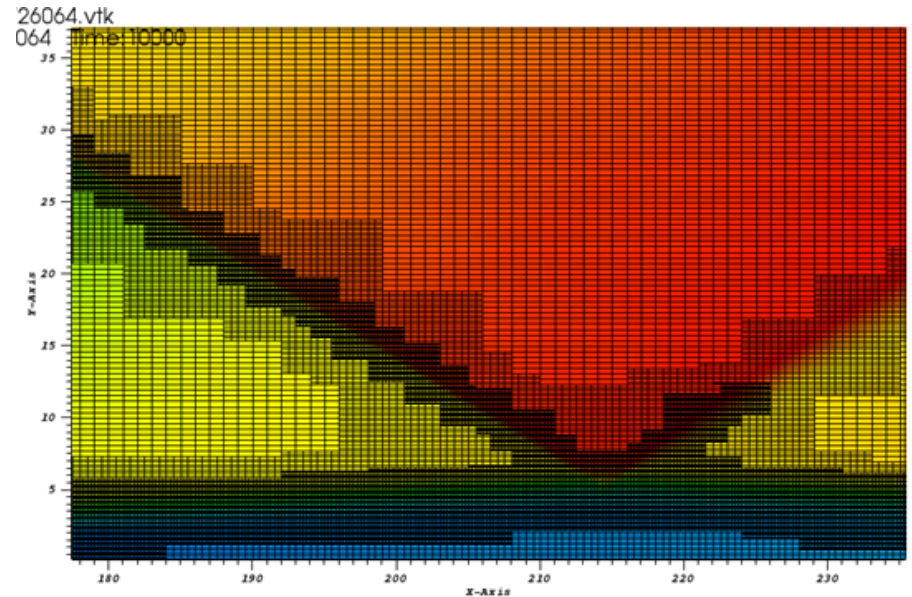
Adaptive Mesh Refinement technique

(Deiterding, 2011)

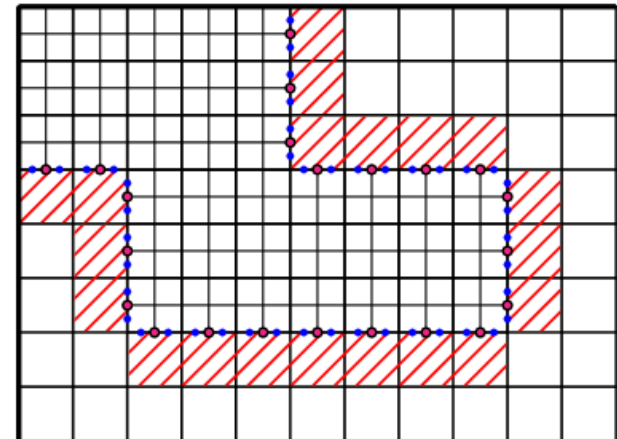
- Consecutive finer levels added dynamically with a patch-wise strategy
- Refinement based on gradient of the physical quantities (e.g. density) – identification of critical (red) zones



Example for a Shock-BL interaction case (density field)

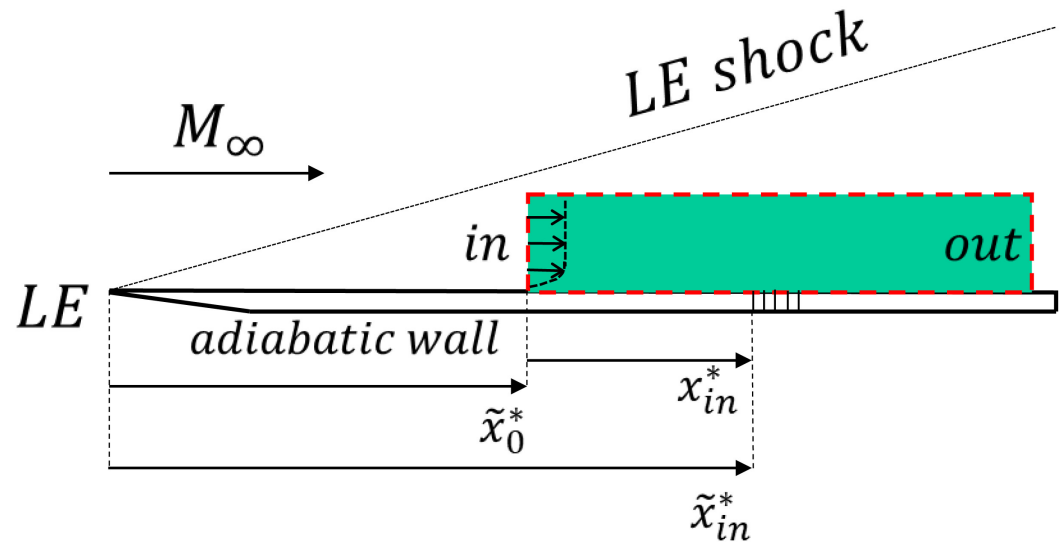


Conservative flux correction at the coarse-fine level interfaces



Flat plate studies: Flow conditions and domain set-up

- $M_\infty = 5$
- $Re_m = 12.6 \times 10^6 \text{ 1/m}$
- $T_\infty^* = 81.7 \text{ K}$
- $T_{0\infty}^* = 490.2 \text{ K}$
- $U_\infty^* = 906 \text{ m/s}$
- $\rho_\infty^* = 0.078 \text{ Kg/m}^3$
- $p_\infty^* = 1.832 \times 10^3 \text{ Pa}$
- $\rho_\infty^* U_\infty^{*2} = 6.4 \times 10^4 \text{ Pa}$
- $\mu_\infty^* = 5.6 \times 10^{-6} \text{ Kg/(m} \cdot \text{s)}$
- $T_w^* = T_{ad}^* = 5.24 T_\infty^*$
- $\tilde{x}_0^* = 127 \text{ mm}$
- $\tilde{x}_{in}^* = 182 \text{ mm}$
- $x_{in}^* = 55 \text{ mm}$



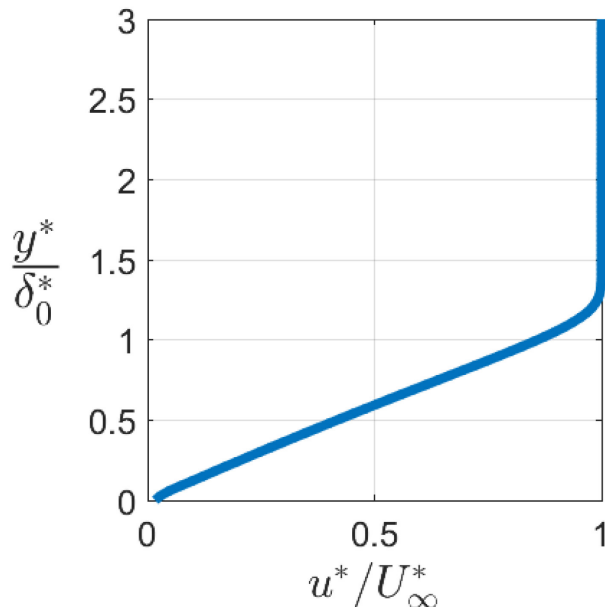
\tilde{x}^* = distance from LE
 x^* = distance from inflow in the domain coordinate system

Initial Inflow BL

The similarity solution gives us the shape of the BL profile to set at the inflow boundary as initial condition.

Hence, the initial condition at the inlet is a similar BL profile with:

- $\delta_{99}^* = 1.25 \text{ mm}$
- displacement thickness $\delta_0^* = 1 \text{ mm}$, $\delta_0^* = \int_0^\infty \left(1 - \frac{\rho^*(y^*)u^*(y^*)}{\rho_\infty^*U_\infty^*}\right) dy^*$



The characteristic length in our computational domain is δ_0^* . Hence, the Reynolds number is:

$$Re_{\delta_0^*} = \frac{\rho_\infty^* U_\infty^* \delta_0^*}{\mu_\infty^*} = 12600$$

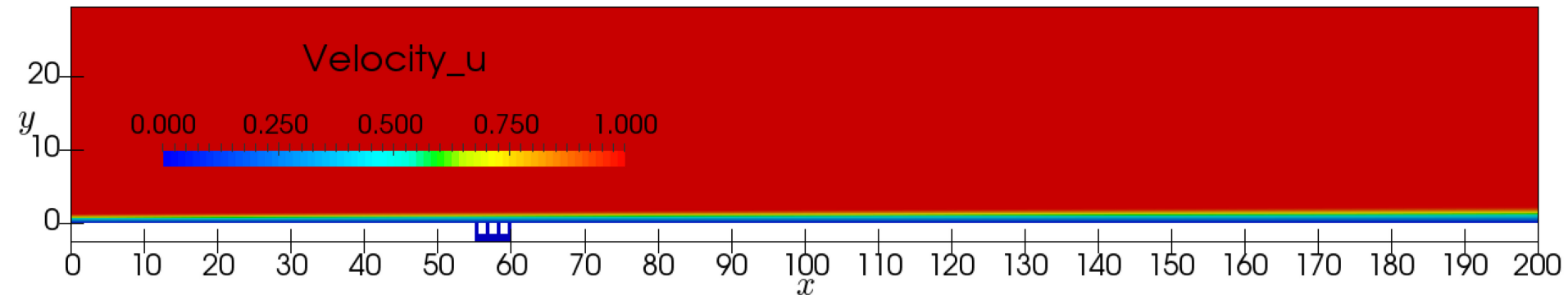
Initialization of the whole domain

From the inflow profile, the displacement thickness of the laminar BL in the initial solution grows in the streamwise direction, following the relation:

$$\frac{\delta^*(\tilde{x}^*)}{\delta_0^*} = \Delta \frac{\sqrt{2Re_{\tilde{x}^*}}}{Re_{\delta_0^*}},$$

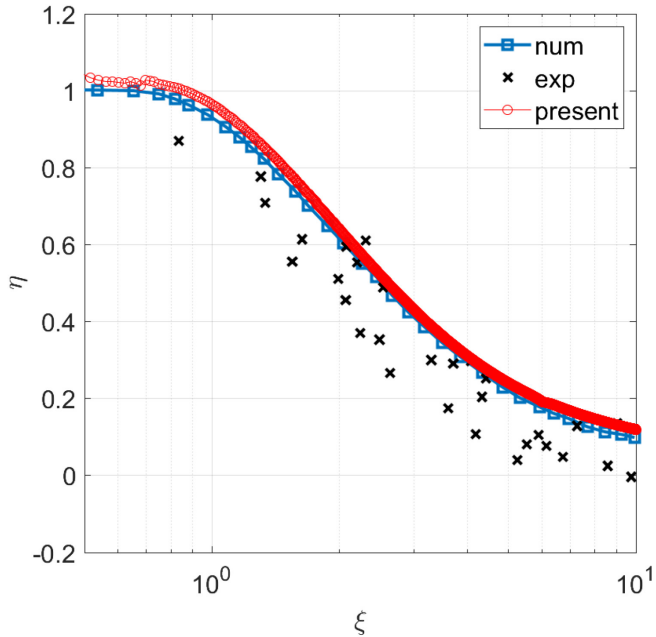
where $\Delta = 8.18$ (for the present case) is a scaling factor from the similarity solution.

The result for the initial state at all the x positions is:

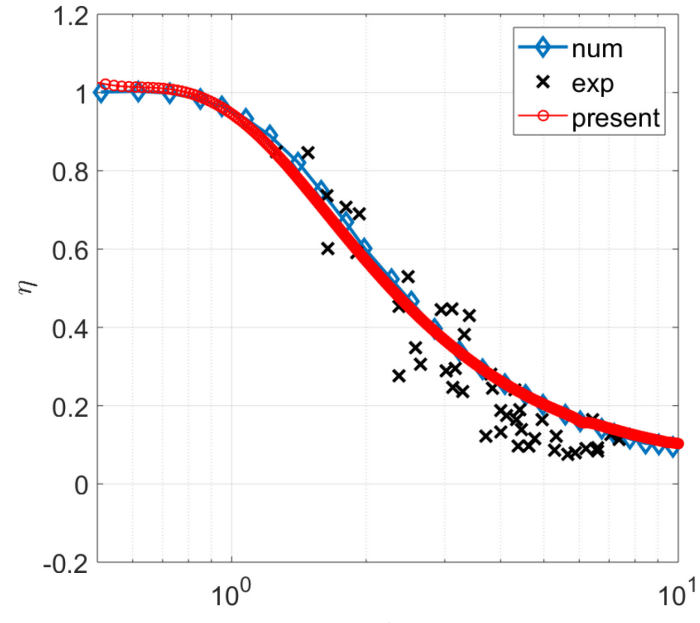


Validation case – slot injection with multicomponent gas effects

Air injection



CO₂ injection



Very good agreement with Keller et al. (2015) results of cooling effectiveness in a Mach 2.6 case

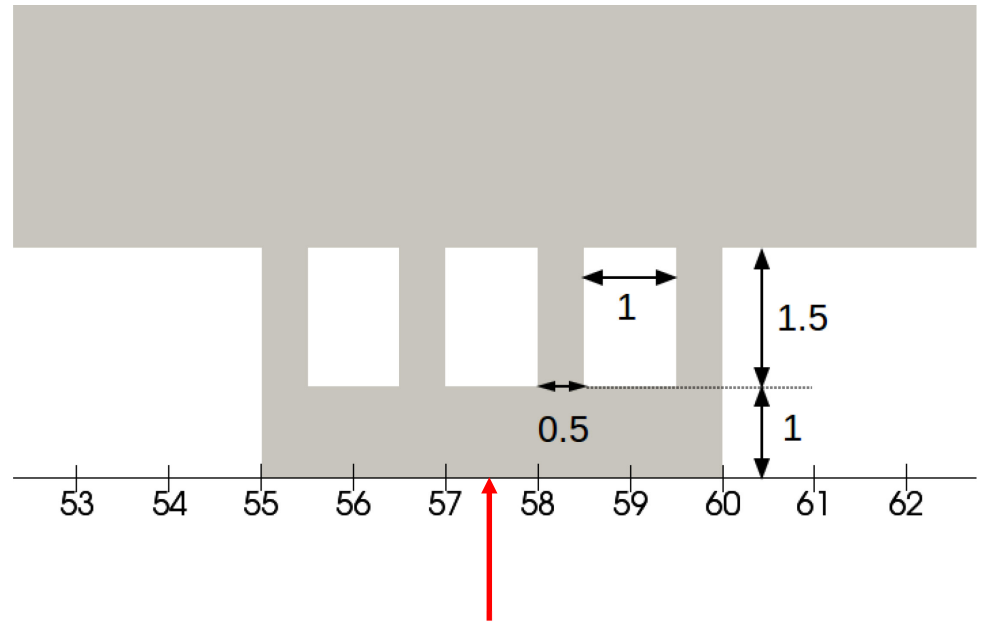


2D results – domain with slots and plenum chamber

Parametric study performed to investigate the effect of the plenum pressure:

- $p_0^* = 1.2p_\infty^* = 2.198 \times 10^3 Pa$
- $p_0^* = 1.5p_\infty^* = 2.748 \times 10^3 Pa$
- $p_0^* = 2.0p_\infty^* = 3.664 \times 10^3 Pa$
- $p_0^* = 3.0p_\infty^* = 5.496 \times 10^3 Pa$

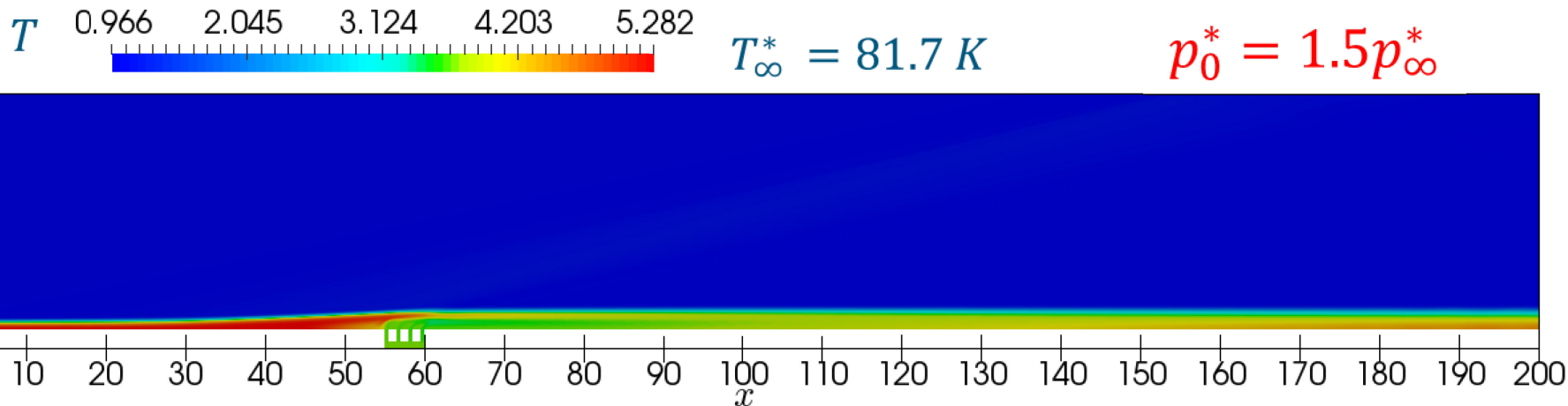
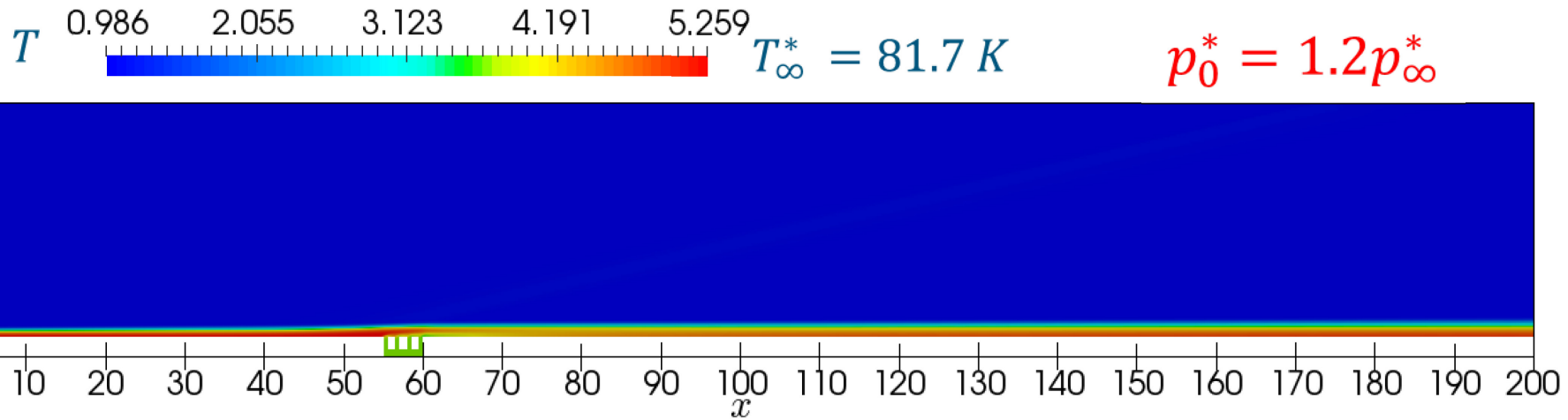
The temperature in the plenum chamber is set
 $T_0^* = 300 K$



Plenum boundary conditions: p_0^*, T_0^*

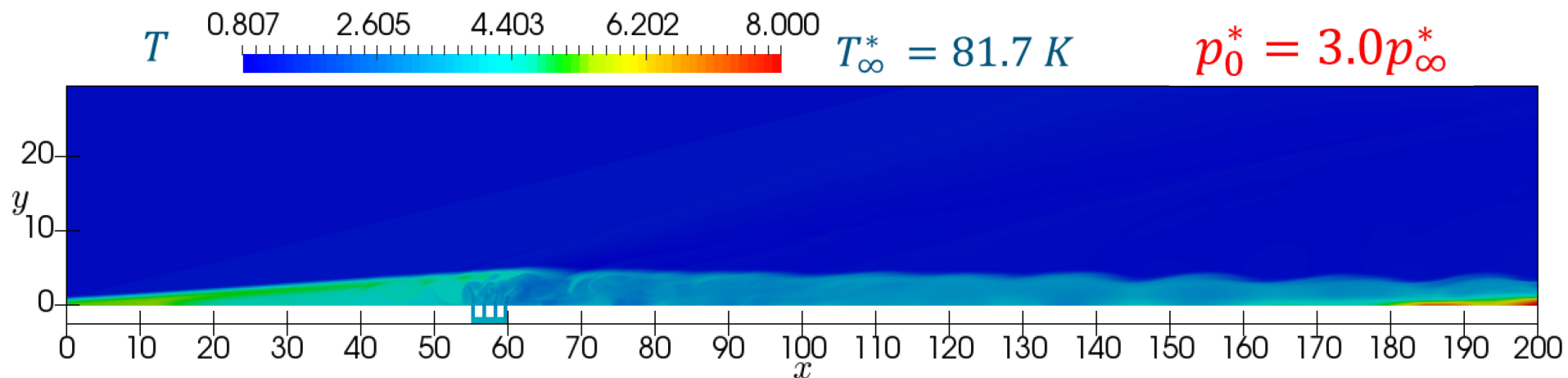
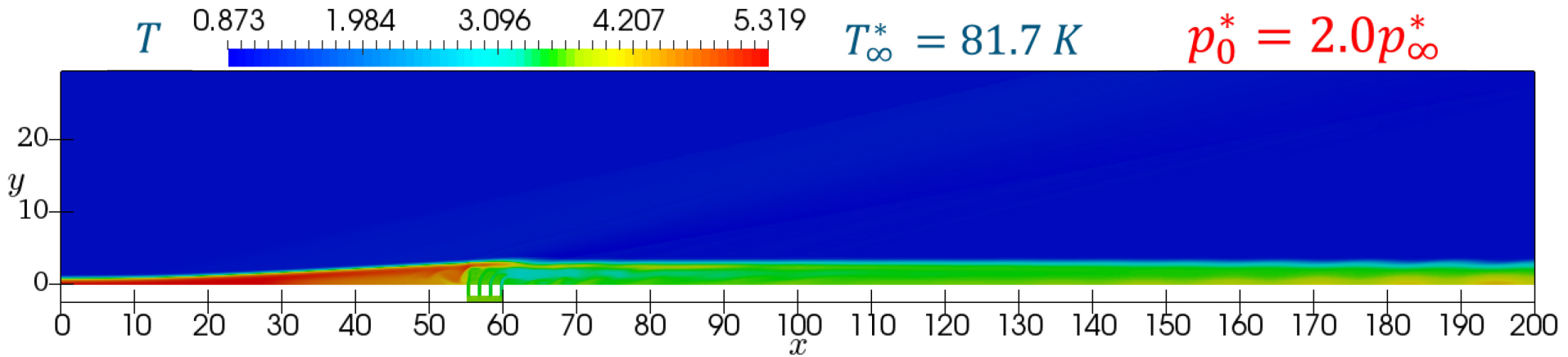
2D results – domain with slots and plenum chamber

Grid size $N_x \times N_y = 800 \times 384$



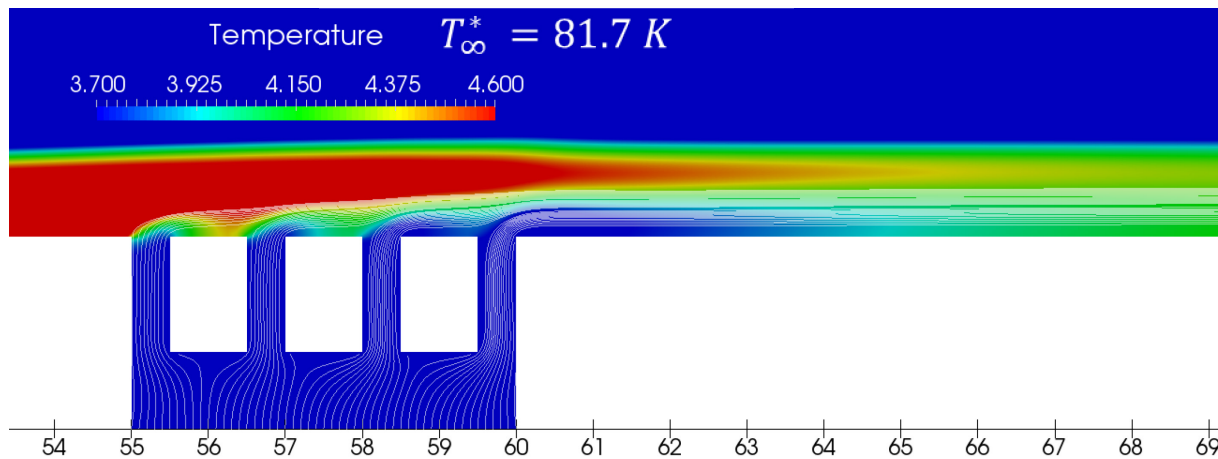
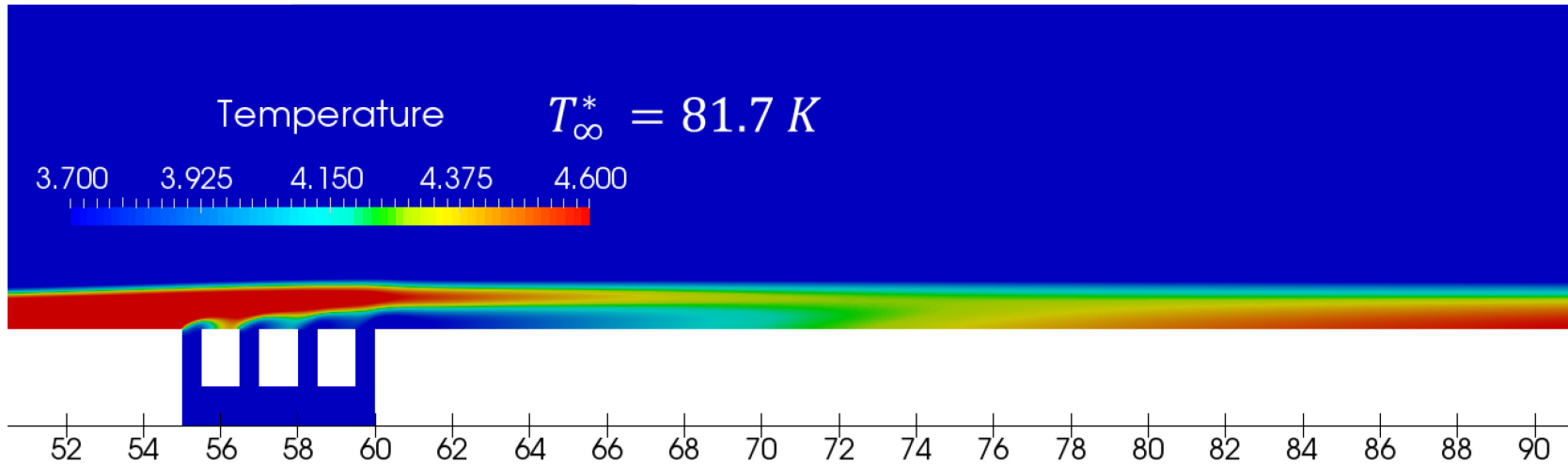
2D results – domain with slots and plenum chamber

Grid size $N_x \times N_y = 800 \times 384$



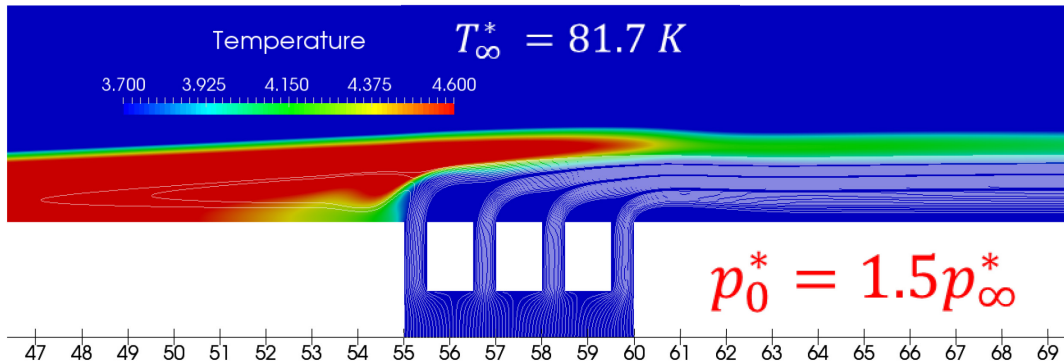
2D results – flow features in the mixing layer

$$p_0^* = 1.2p_\infty^*$$

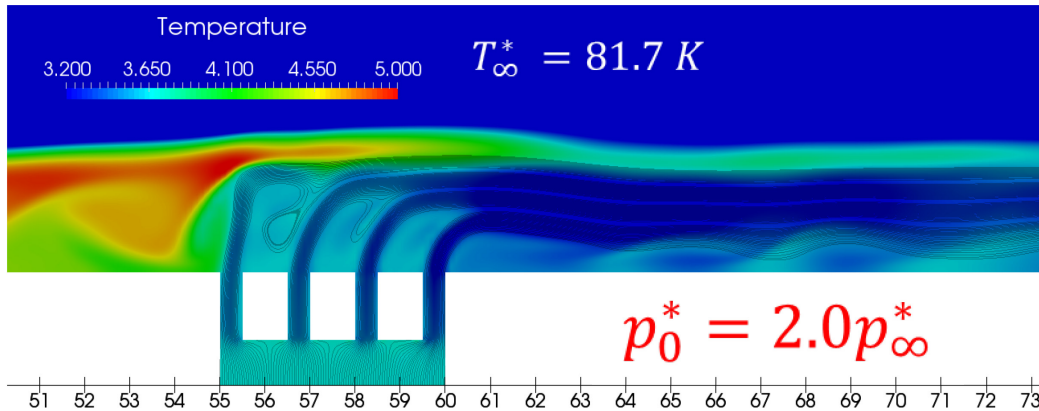


Thin film of cold fluid adjacent to the wall – laminar mixing layer – but limited extent of the cooled region

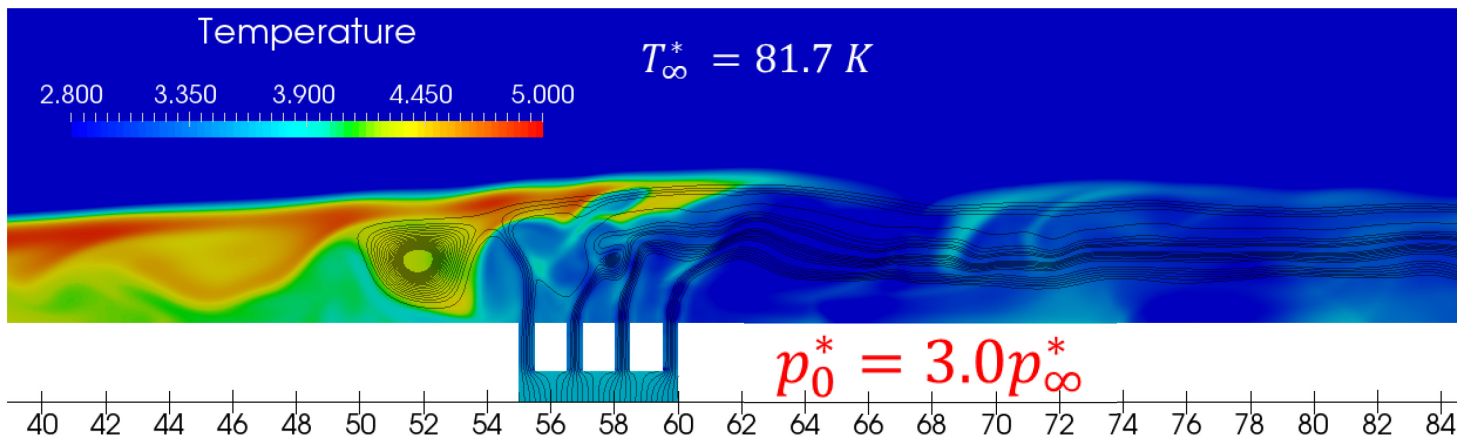
2D results – flow features in the mixing layer



Thicker laminar cold layer and recirculation in the upstream region



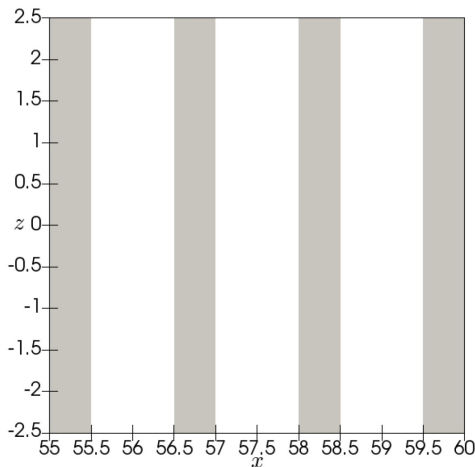
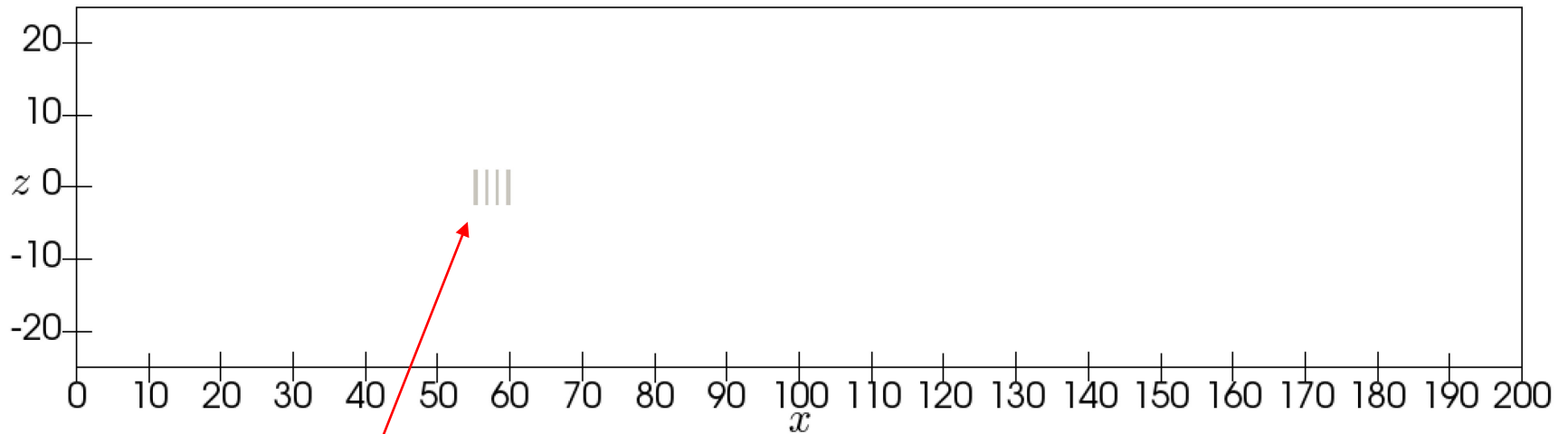
Cold fluid affecting the upper region of the BL - strong waves near the wall convected downstream



Vortical mixing layer with non-uniform T - strong effects upstream

3D flat plate with blowing through slots

Grid size (base level) $N_x \times N_y \times N_z = 800 \times 384 \times 100$



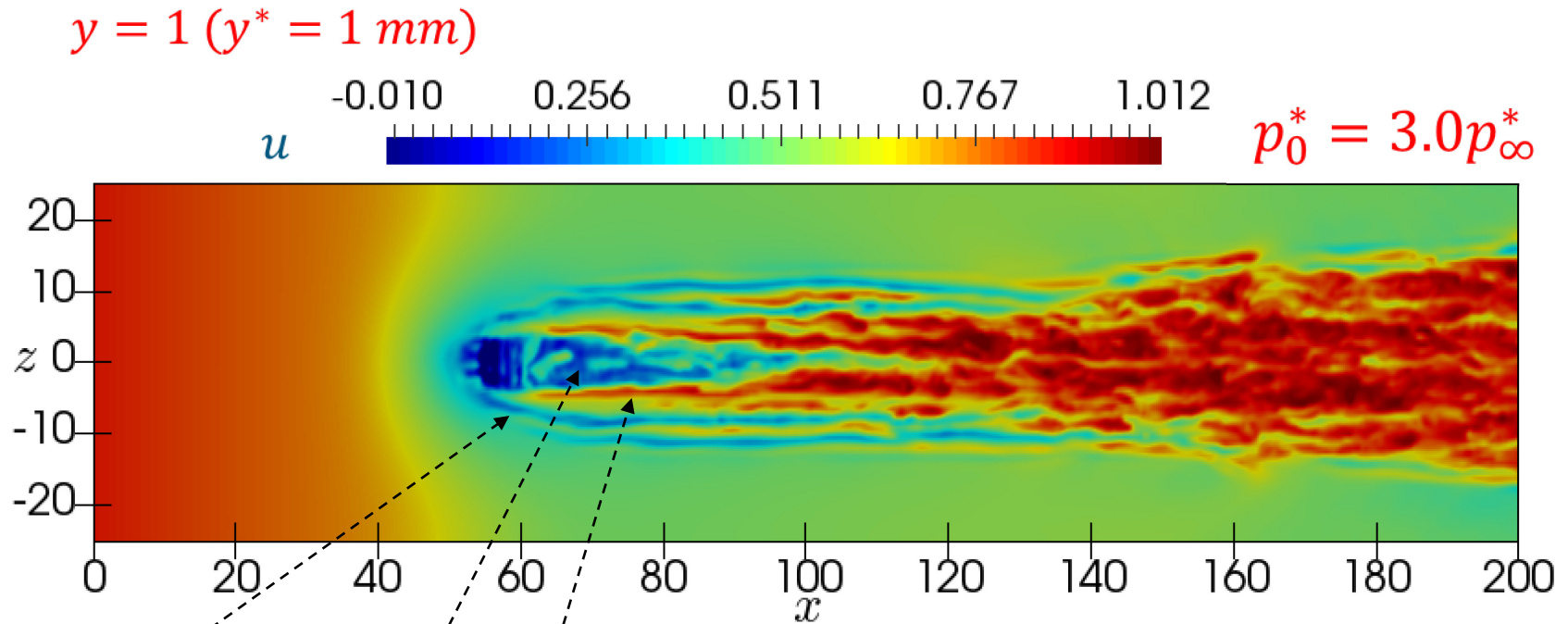
Domain size $L_x \times L_y \times L_z = 200 \times 32 \times 50$

Width of the slot region = 5 mm

Minimum cell sizes $\Delta x = 0.125$ mm, $\Delta y = 0.0415$ mm, $\Delta z = 0.25$ mm (with 2 grid levels)

Simulation run with 480 cores on Iridis 4 cluster (Soton HPC facility)

3D flat plate with blowing through slots



Horseshoe
vortices
(low-velocity
streaks)

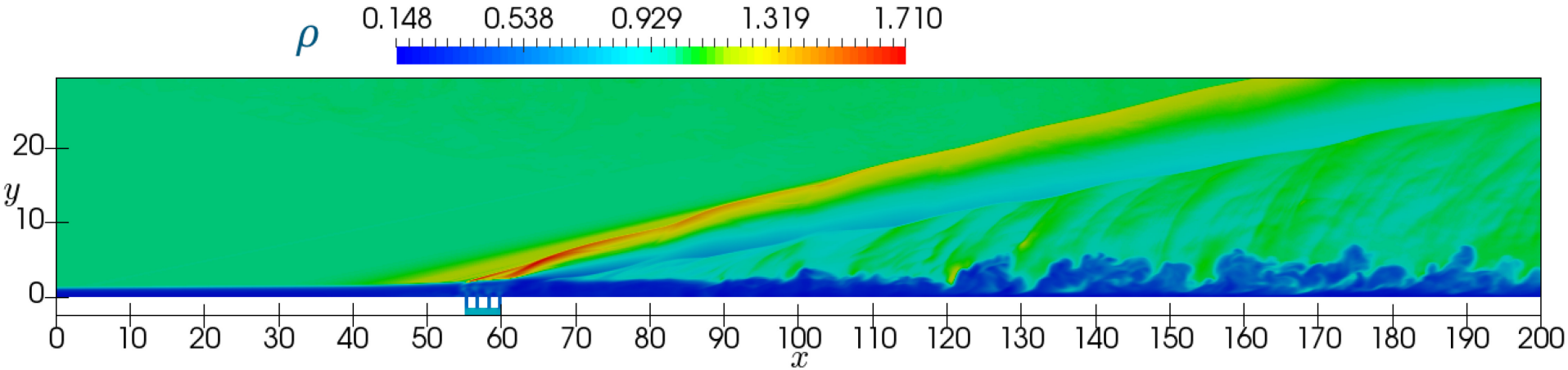
wake

Edge vortices
(high-velocity
streaks)

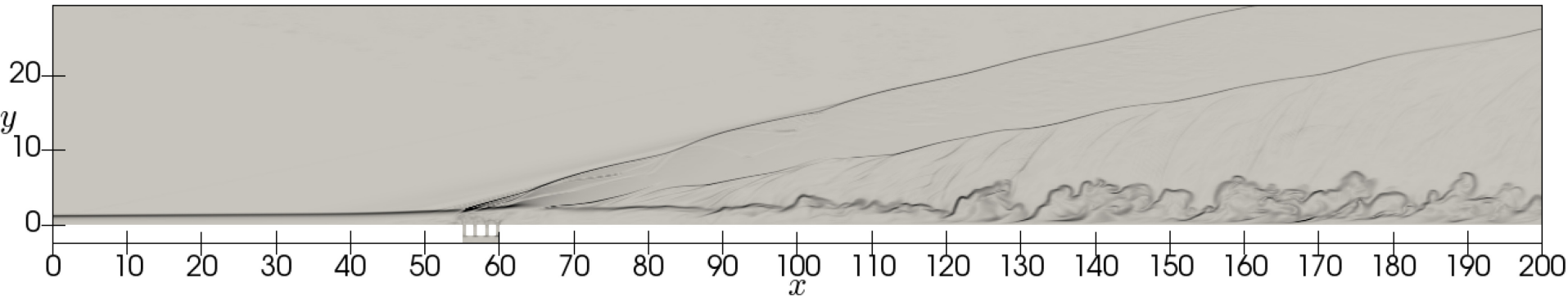
- Transition induced by breakdown of the main edge vortices downstream of $x = 90$ ($x^* = 90$ mm, $\tilde{x}^* = 217$ mm)
- Wedge-shaped transition front spreading downstream

3D flat plate with blowing through slots

Centerline plane ($z = 0$)



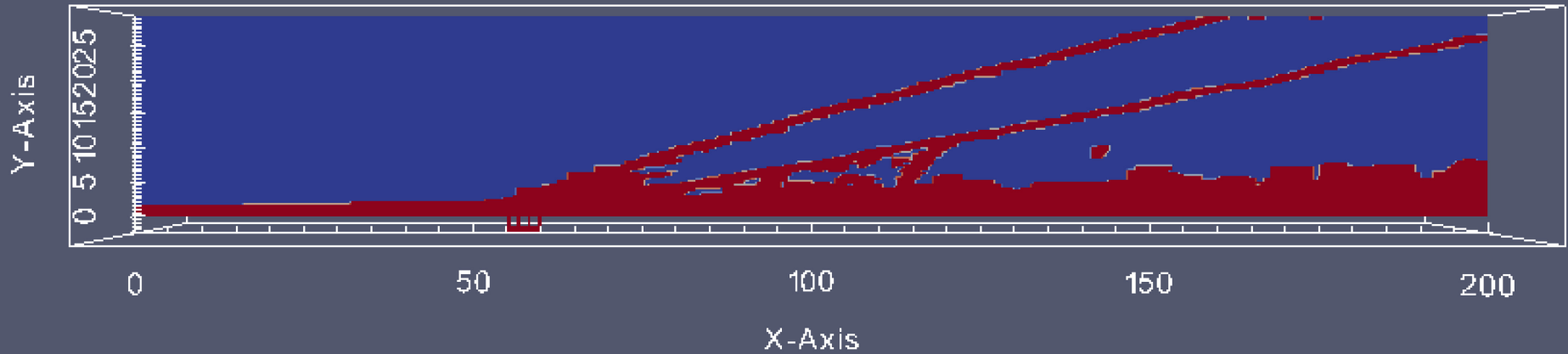
Schlieren



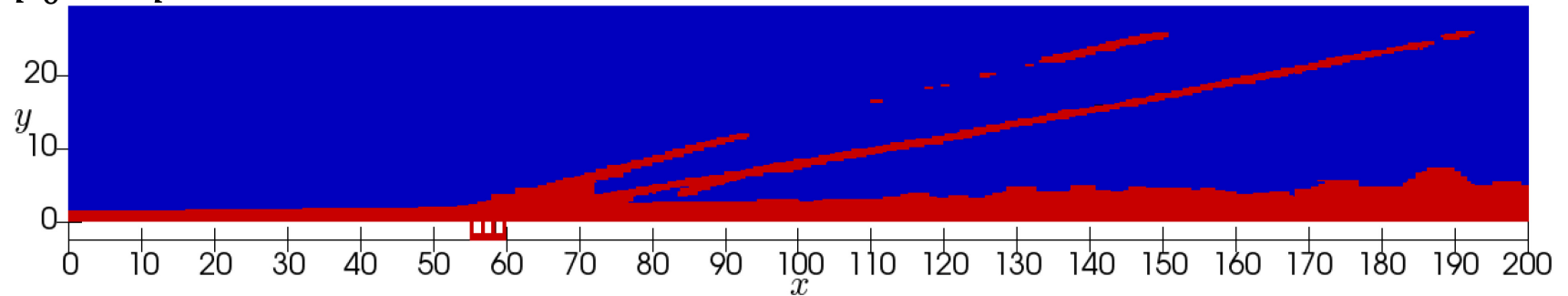
- Smaller size of the separation bubble, and front shock very close to injection slots (due to 3D effects), compared to the 2D case
- Evident acoustic waves generated by the turbulent BL downstream

3D results – grid levels

$p_0^* = 3p_\infty^*$ Centerline plane ($z = 0$)



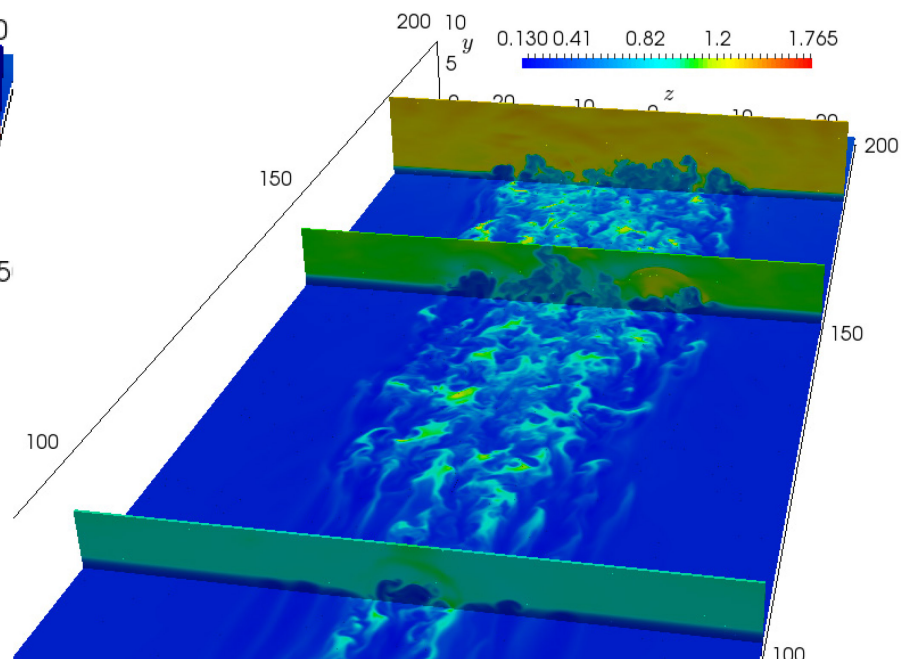
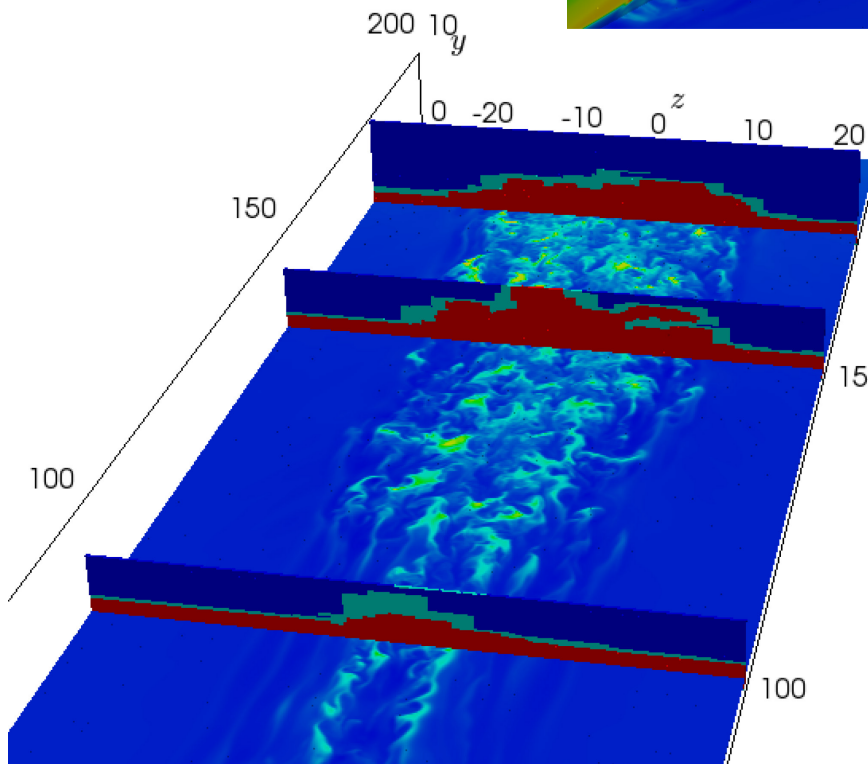
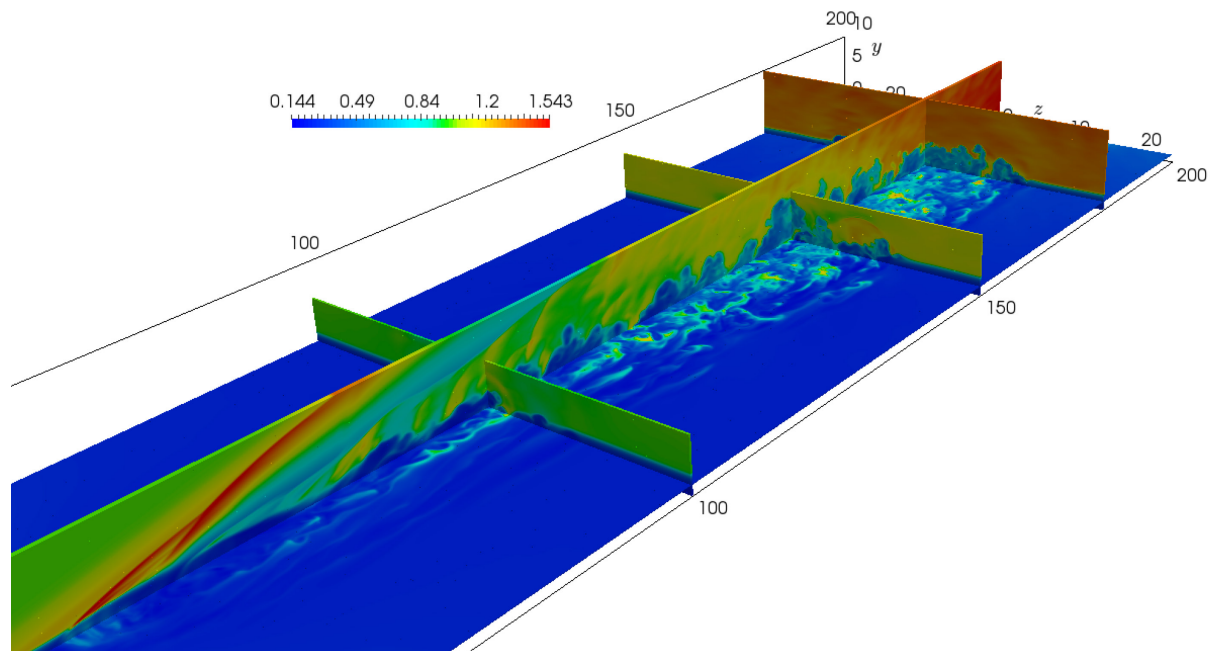
$p_0^* = 2p_\infty^*$



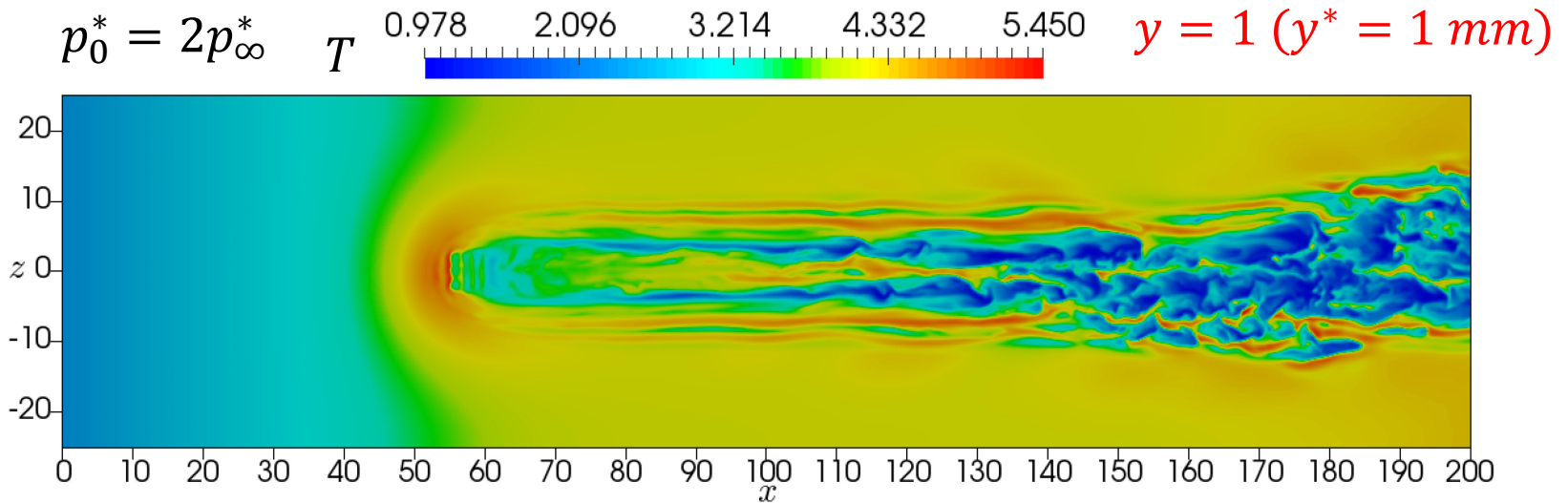
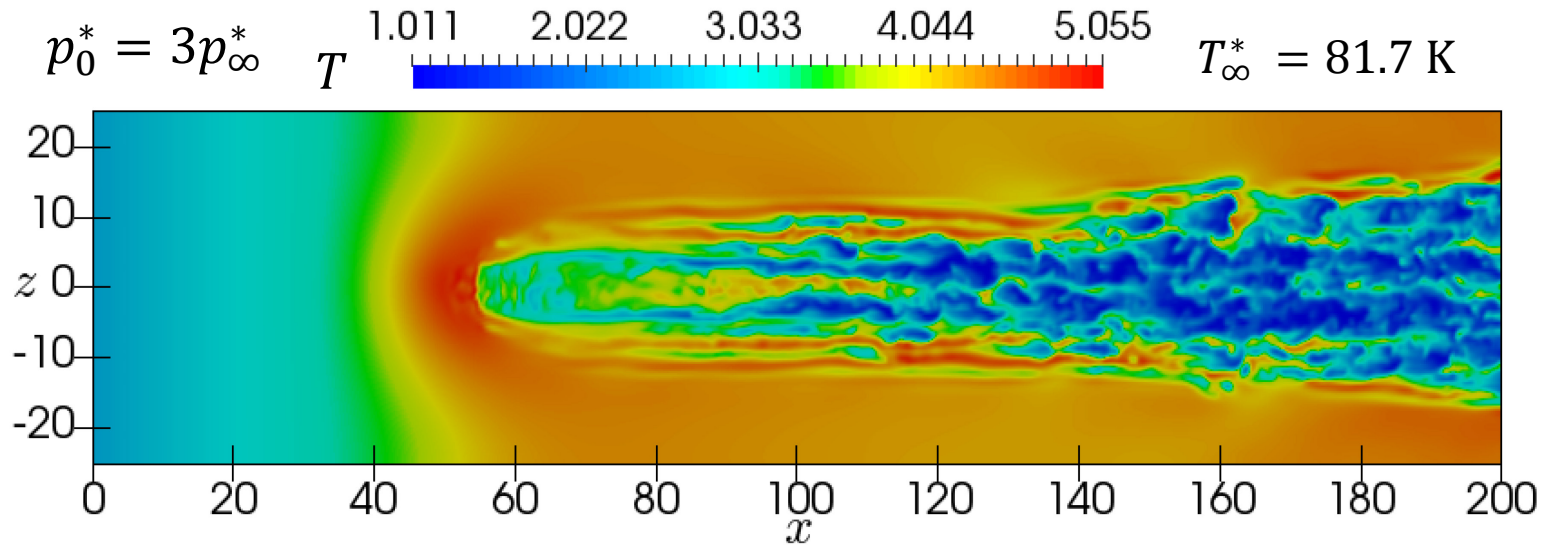
3D results

Right, bottom right: density field

Left, bottom: AMR levels



3D results - effect of plenum pressure

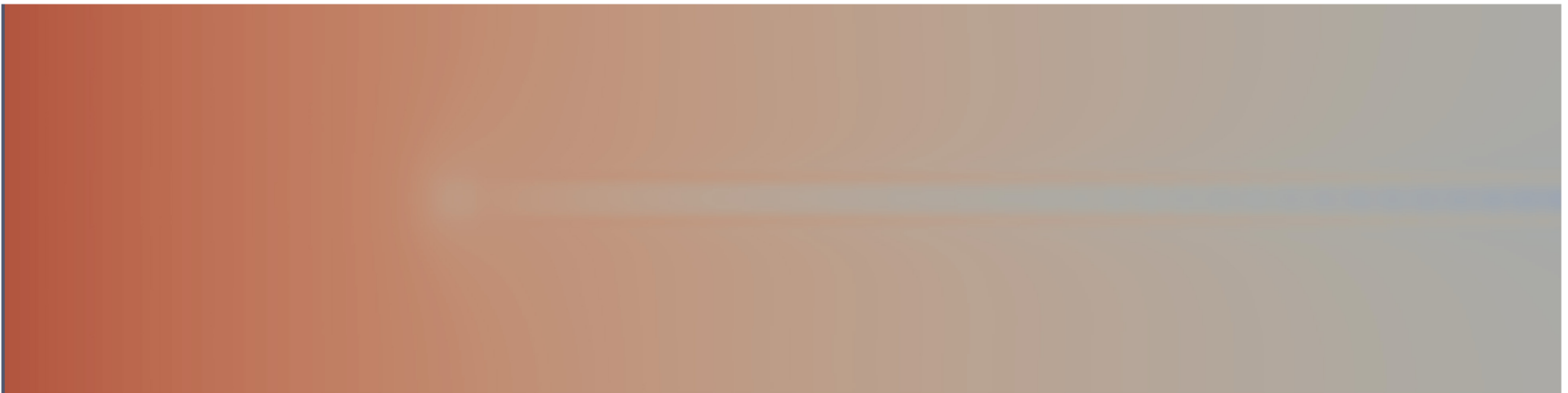


Effect of plenum pressure – relaminarisation for lower plenum pressures

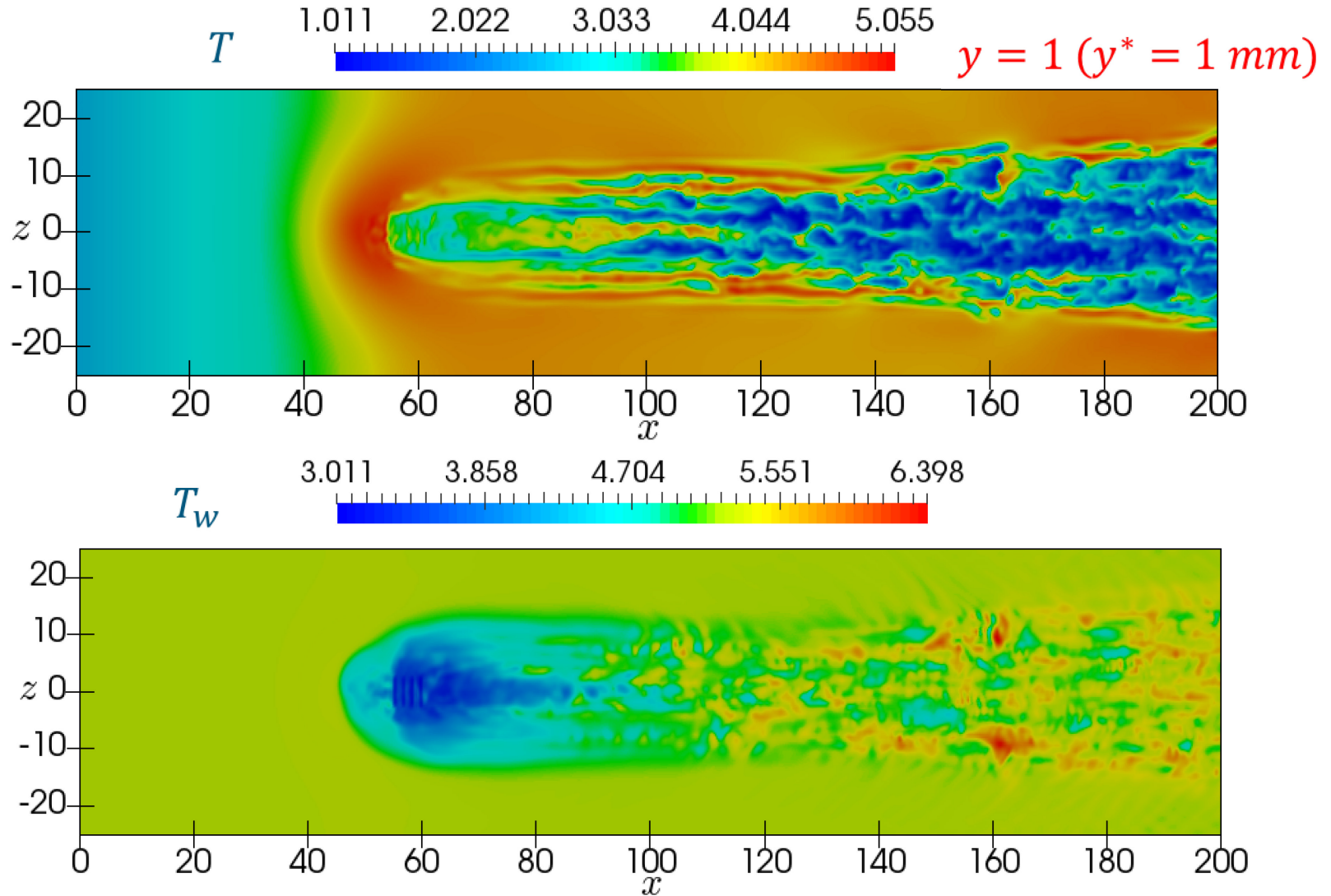
$$p_0^* = 1.5p_\infty^*$$



$$p_0^* = 1.2p_\infty^*$$

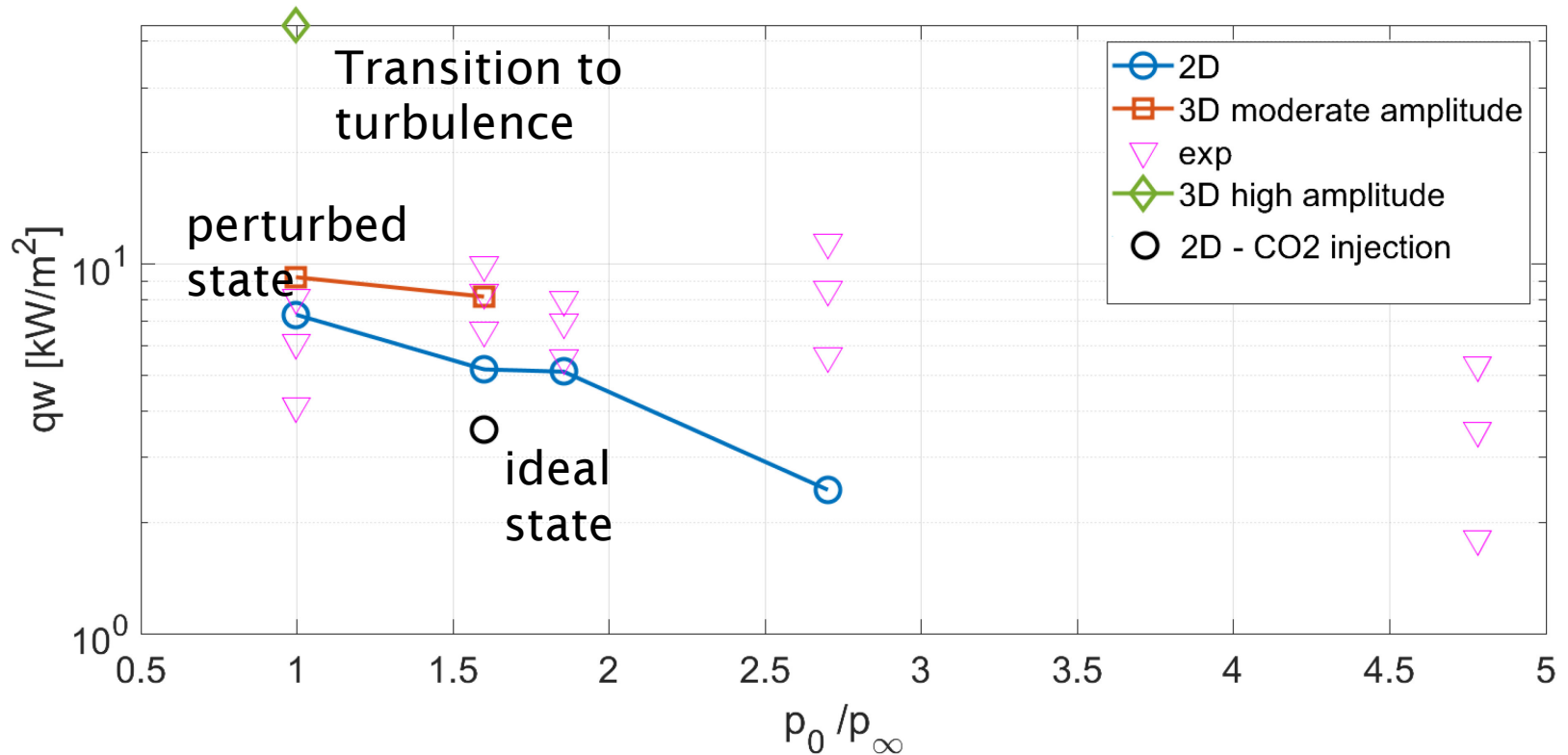


3D flat plate with blowing through slots



- Cooling performed mainly at the slot sides and along the wake
- Limited streamwise extent of the cooled region due to transition to turbulence 24

Slotted flat plate – Oxford exp. - assessment of disturbance effects on BL

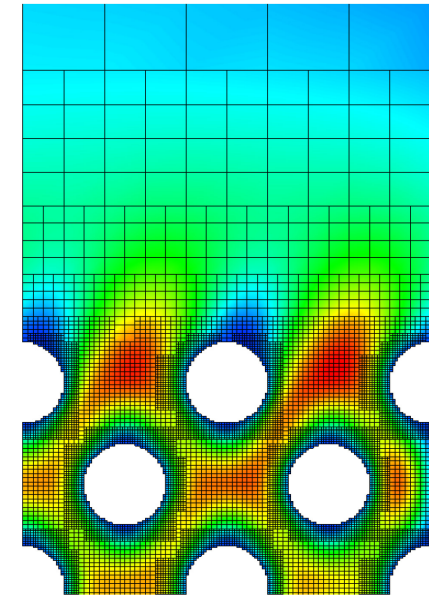
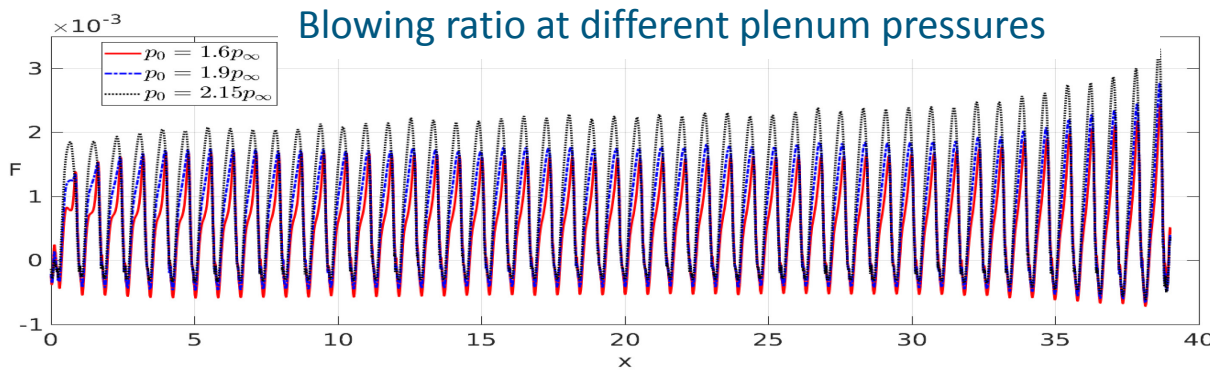
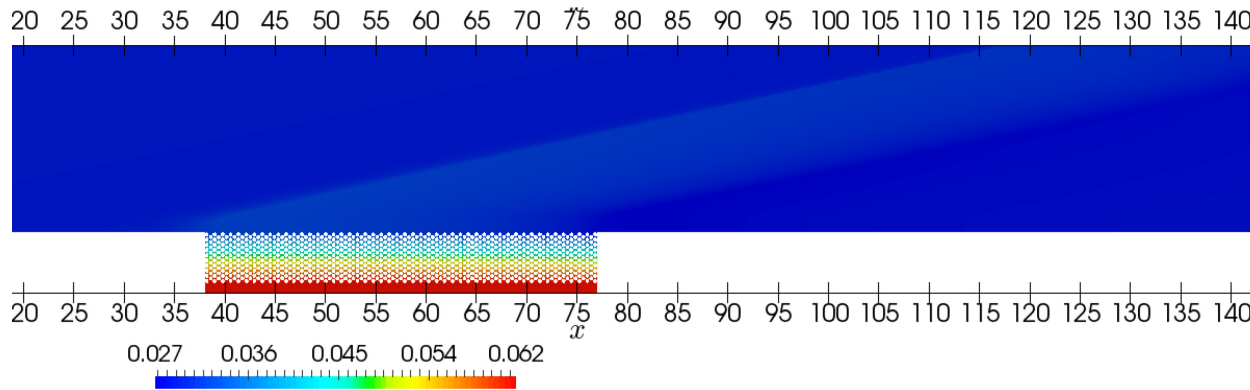


Simulations suggest that transition to turbulence has not occurred yet in the experiment, but the boundary layer is actually in a perturbed state, characterized by disturbance excitation and growth

Modelling of porous media experiment

- Original project proposal assumed grain structures of $>50\mu\text{m}$
- Current material has grains $<2\mu\text{m}$ (cost of DNS increases by factor approx. $25^4=390625$)
- New approach: model the porous media flow using regular sphere/cylinder arrays of resolvable mesoscopic size

Cylinders with radius of $200\mu\text{m}$, pressure contours



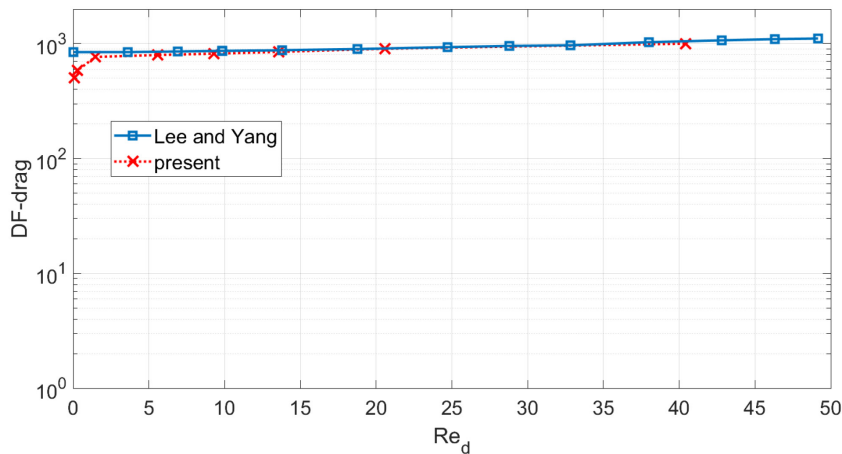
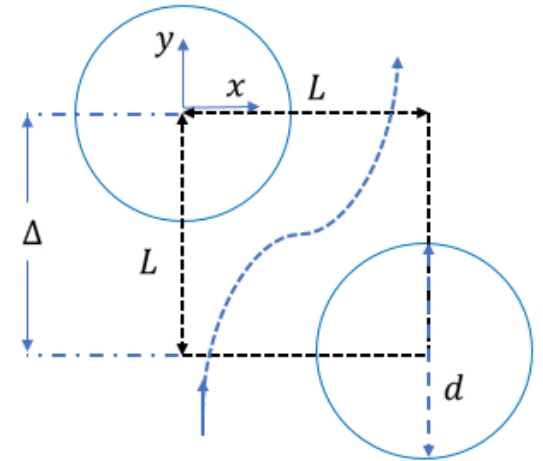
Automatic adaptive mesh (vertical velocity)

Darcy-Forchheimer multiscale model

$$D - F = \frac{d^2}{K} + FRe_d = Re_c \left(\frac{d}{L} \right)^2 \frac{1}{q} \quad Re_c = \frac{\rho U_c L}{\mu} \quad U_c = \sqrt{\frac{\Delta p}{\rho}} \quad Re_d = \frac{qd}{\mu} = Re_c \left(\frac{d}{L} \right) q$$

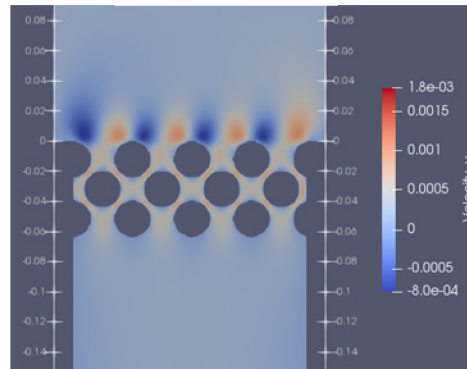
$$q = \frac{1}{\rho U_c L} \int_0^L \rho u dx \quad \frac{d}{L} = f(\varepsilon)$$

- Objective: represent the Darcy-Forchheimer drag of micro-structured material with larger cylinders
- Preliminary study follows approach of Lee and Yang (1997)



d

$d = 48\mu\text{m}$



Can vary d and maintain q

Matching with experiment in terms of blowing ratio, and rescaling to higher pore sizes

Quantifying integrated blowing ratio solution (q) for the different pore/particle sizes:

$$Re_C = 1.67$$

$$d = 12 \mu m \rightarrow q = 3.8 \times 10^{-3}$$

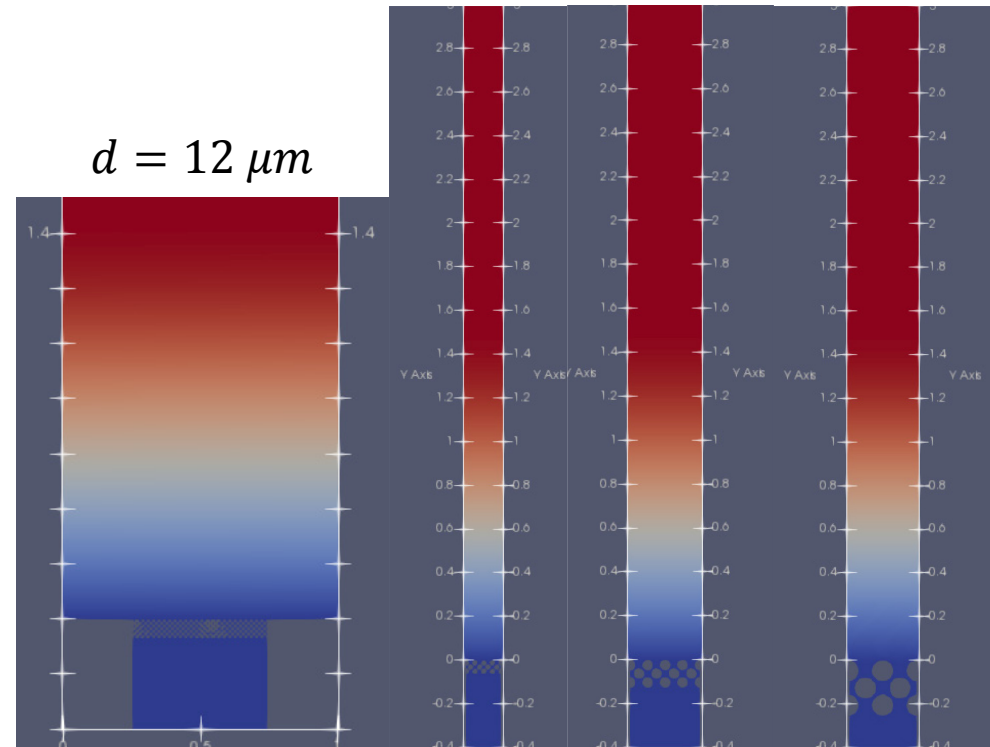
$$d = 24 \mu m \rightarrow q = 3.7 \times 10^{-3}$$

$$d = 48 \mu m \rightarrow q = 3.6 \times 10^{-3}$$

$$d = 96 \mu m \rightarrow q = 3.8 \times 10^{-3}$$

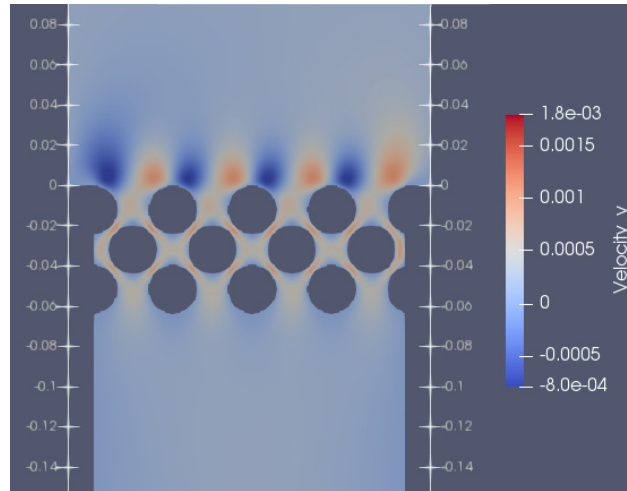
Simulation results show rescaling capability from very small pore sizes to higher scales in terms of the D-F behaviour

$d = 24 \mu m$ $d = 48 \mu m$ $d = 96 \mu m$

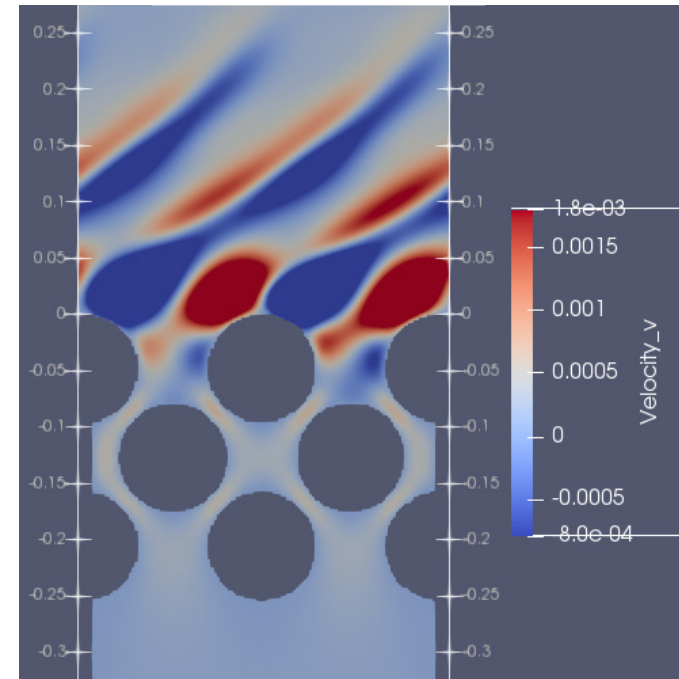


Effect of pore size on the flow features

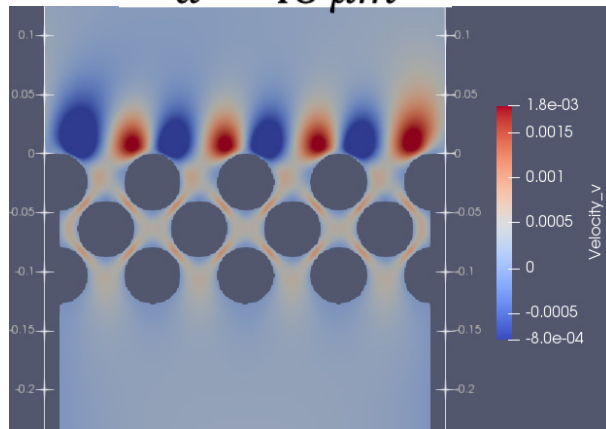
$d = 24 \mu\text{m}$



$d = 96 \mu\text{m}$



$d = 48 \mu\text{m}$



-very similar patterns of the D-F behavior within the porous layer
-stronger shear layer at the pore edges for higher sizes – and generated acoustic waves

Conclusions

- We have successfully validated a hybrid 6th order hybrid WENO/CD method in the AMROC framework for DNS of hypersonic boundary layers with wall injection
- The method is efficient, robust and runs well on massively parallel systems
- Additional modelling challenges have to come to light
- 3D simulations with disturbances (of the most unstable mode found) show better agreement with experimental results for moderate disturbances, suggesting that the available experiment is still in a perturbed pre-transitional state
- Multiscale model required to enable mesoscopic simulations with idealized porous material
- Rescaling capabilities at higher pore sizes have been demonstrated and assessed, however effects of the particle size on the near-wall BL are observed